

## GENERALIZED ADDITIVE MODELLING OF MIXED DISTRIBUTION MARKOV MODELS WITH APPLICATION TO MELBOURNE'S RAINFALL

ROB J. HYNDMAN<sup>1\*</sup> AND GARY K. GRUNWALD<sup>2</sup>

*Monash University and University of Colorado*

### Summary

The paper considers the modelling of time series using a generalized additive model with first-order Markov structure and mixed transition density having a discrete component at zero and a continuous component with positive sample space. Such models have application, for example, in modelling daily occurrence and intensity of rainfall, and in modelling numbers and sizes of insurance claims.

The paper shows how these methods extend the usual sinusoidal seasonal assumption in standard chain-dependent models by assuming a general smooth pattern of occurrence and intensity over time. These models can be fitted using standard statistical software. The methods of Grunwald & Jones (2000) can be used to combine these separate occurrence and intensity models into a single model for amount. The models are used to investigate the relationship between the Southern Oscillation Index and Melbourne's rainfall, illustrated with 36 years of rainfall data from Melbourne, Australia.

*Key words:* binary time series; droughts; dry spells; gamma time series; generalized additive model; generalized linear model; Markov model; mixture distribution; non-Gaussian time series; southern oscillation index.

### 1. Introduction

Time series with a mixed density composed of a discrete component at zero and a continuous component on the positive real line commonly occur with meteorological and environmental data where there may be no recordable level of precipitation or pollutant at some times. They also occur in some business contexts such as insurance claims and non-recurrent expenditure.

Most of the previous discussion about modelling such data has concentrated on modelling daily rainfall occurrence and amounts. In this paper, we also use some rainfall data in illustration, although our methods are generally applicable to all such time series with mixed density.

One approach developed by Stern & Coe (1984) uses generalized linear models (GLMs; see McCullagh & Nelder, 1989) to model rain occurrence (probability) and intensity (amount

---

Received December 1998; revised September 1999; accepted September 1999.

\* Author to whom correspondence should be addressed.

<sup>1</sup> Department of Econometrics and Business Statistics, Monash University, Clayton VIC 3168, Australia.

e-mail: rob.hyndman@buseco.monash.edu.au

<sup>2</sup> Department of Preventive Medicine and Biometrics, University of Colorado Health Sciences Center, Denver, CO 80262, USA.

*Acknowledgments.* Gary Grunwald and Rob Hyndman were supported by Australian Research Council grants. Much of the work by Gary Grunwald was completed when he was in the Department of Statistics, University of Melbourne. The work by Rob Hyndman was done while he was visiting the Department of Statistics, Colorado State University. The authors thank Lynda Chambers of the Bureau of Meteorology and two anonymous referees for their helpful comments.

when it rains). These methods are effective in describing typical rainfall patterns throughout the year, but they assume the same seasonal pattern for each year and thus are not capable of modelling droughts, trends, or other non-seasonal effects. They also result in separate models for occurrence and intensity rather than a single model for rainfall amount.

Recent developments in statistical methodology have made it possible to formulate and estimate more complex models. In this paper we use the generalized additive models (GAMs) of Hastie & Tibshirani (1990) to relax the assumption that each year follows the same seasonal pattern, and the Markov models for mixed distributions (Grunwald & Jones, 2000) to combine the separate occurrence and intensity models into a single model for amount.

To illustrate our model and estimation methods, we use daily rainfall data from Melbourne, Australia (the Melbourne city station, 86071) for the period 1 January 1963 to 30 September 1998. During this period rainfall was recorded on 39.8% of the 13 057 days. We show that, for this series, rainfall is influenced by several factors including seasonality, drought, and rainfall occurrence and intensity the preceding day.

## 2. The model

Let  $Y_t$  be a random variable denoting the series at time  $t$ ,  $t = 1, \dots, n$ . This is referred to as the *amount process*. The distribution of  $Y$  is assumed to be a mixture comprising a discrete component at  $y = 0$  and a continuous component for  $y > 0$ .

Let  $q_t(y | \mathbf{X}_t = \mathbf{x}_t)$  denote the transition ‘density’ for  $Y_t$  where  $\mathbf{X}_t$  denotes a vector of covariates including  $Y_{t-1}$ , and possibly other explanatory variables. (The term ‘density’ is used loosely here because the distribution is a mixture of discrete and continuous components.) Following Stern & Coe (1984) and others, we introduce the occurrence and intensity processes to simplify expressions for  $q$ .

The *occurrence process* is  $J_t = 1$  if  $Y_t > 0$  and  $J_t = 0$  otherwise. Thus it is an indicator process of whether  $Y_t$  is positive. The *intensity process* is defined to be  $W_t = Y_t$  if  $Y_t > 0$  and missing otherwise. The bivariate random variable  $(Y_t, J_t)$  is assumed to be Markov order  $p$ .

Thus,  $J_t$  has conditional Bernoulli distribution with  $\pi_t(\mathbf{x}_t) = \Pr(J_t = 1 | \mathbf{X}_t = \mathbf{x}_t)$ . We use the logit link function so that

$$\pi_t(\mathbf{x}_t) = \ell(\mu_t(\mathbf{x}_t)) \quad \text{where} \quad \ell(u) = \frac{e^u}{1 + e^u},$$

$$\mu_t(\mathbf{x}_t) = \alpha_0 + \sum_{k=1}^p (\alpha_k J_{t-k} + g_k(y_{t-k})) + \sum_{i=p+1}^r g_i(x_{i-p,t}) + g_{r+1}(t),$$

$\mathbf{X}_t = (J_{t-1}, \dots, J_{t-p}, Y_{t-1}, \dots, Y_{t-p}, X_{1t}, \dots, X_{r-p,t})^\top$  is a vector of covariates, and each  $g_i$  ( $i = 1, 2, \dots, r+1$ ) is a smooth function. We can generalize this model further by allowing some interaction between the covariates.

Let the intensity process  $W_t$  have continuous conditional density  $f_t(w | \mathbf{X}_t)$  for  $w > 0$  and 0 otherwise. We assume that  $f_t$  is a gamma density with mean  $v_t(\mathbf{x}_t)$  and log link function so that

$$\log(v_t(\mathbf{x}_t)) = \beta_0 + \sum_{k=1}^p (\beta_k J_{t-k} + h_k(y_{t-k})) + \sum_{i=p+1}^r h_i(x_{i-p,t}) + h_{r+1}(t),$$

where each  $h_i$  ( $i = 1, 2, \dots, r+1$ ) is a smooth function. The shape parameter of the density  $f_t$  is assumed to be constant for all  $t$  and  $\mathbf{x}_t$ . Note that we could replace the gamma density assumption by some other appropriate density such as the log-normal which was used by Katz & Parlange (1995). Or, more generally, we could estimate  $f_t$  non-parametrically using the methods of Hyndman, Bashtannyk & Grunwald (1996) and Hyndman & Yao (1998). However, in this paper we use the gamma density.

The transition density of  $Y_t$  can now be written as

$$q_t(y | \mathbf{X}_t = \mathbf{x}_t) = (1 - \pi_t(\mathbf{x}_t))\delta_0(y) + \pi_t(\mathbf{x}_t)f_t(y | \mathbf{x}_t), \quad (2.1)$$

where  $\delta_0(y)$  denotes a Dirac delta function with support zero. Properties of  $Y_t$  such as moments conditional on  $Y_{t-1}$  can be found as in Aitchison (1955). We give such results as we use them below.

Following Grunwald & Jones (2000), we assume that  $\pi_t(\mathbf{x}_t)$  and  $f_t(w | \mathbf{x}_t)$  have no common model terms, so that the likelihood admits a simple factorization.

The above model generalizes the model of Grunwald and Jones in several ways. We allow the dependence of  $Y_t$  on  $t$  and  $\mathbf{X}_t$ , and of  $J_t$  on  $t$  and  $\mathbf{X}_t$ , to be nonlinear and estimate it non-parametrically using a GAM. In particular, we do not assume the same seasonal patterns recur every year, thus providing the facilities to model unusual events (such as droughts if  $Y_t$  denotes rainfall).

Note that intervention effects such as changes in measurement or relocation of a recording station, which in Grunwald & Jones (2000) needed to be modelled explicitly using dummy variables, can now be modelled by  $g_{r+1}(t)$  and  $h_{r+1}(t)$ , and need not be included in the model separately. However, these effects are now included in a smooth form, so if the effect is of real interest in its own right, or if it is expected to be discontinuous in effect, inclusion of a separate term may be useful.

One by-product of our model is a natural method for producing seasonally adjusted estimates of probabilities of occurrence and mean intensity.

### 3. Estimation

The fitting of this model requires estimation of  $\alpha_j$  and  $\beta_j$  ( $j = 0, \dots, p$ ), and the functions  $g_i$  and  $h_i$  ( $i = 1, \dots, r+1$ ). The mixed transition density is not of a standard form, so standard methods and software are not available for doing this. However, Grunwald & Jones (2000) show that for GLMs, if it is assumed that there are no common parameters in the occurrence and intensity models, the Markov likelihood function for  $(y_2, \dots, y_n)$  conditional on  $Y_1 = y_1$  as found from (2.1), factorizes into separate parts for the occurrence and intensity models. Thus, the overall likelihood is maximized by the estimates of  $\alpha_j$ ,  $\beta_j$ ,  $g_i$  and  $h_i$  which maximize the occurrence and intensity models separately. The same argument holds for GAMs. Because the occurrence and intensity models have standard transition densities (binary and gamma, respectively), the standard methods and software of GAMs can be used.

The functions and parameters in the separate models can be estimated using GAMs with any non-parametric smoothing method including moving averages, locally weighted polynomials such as loess (Cleveland, Grosse & Shyu, 1992), smoothing splines (Green & Silverman, 1994) or penalized regression splines (Eilers & Marx, 1996). The present implementation of generalized additive modelling in S-PLUS allowed loess or spline smoothing; we chose the

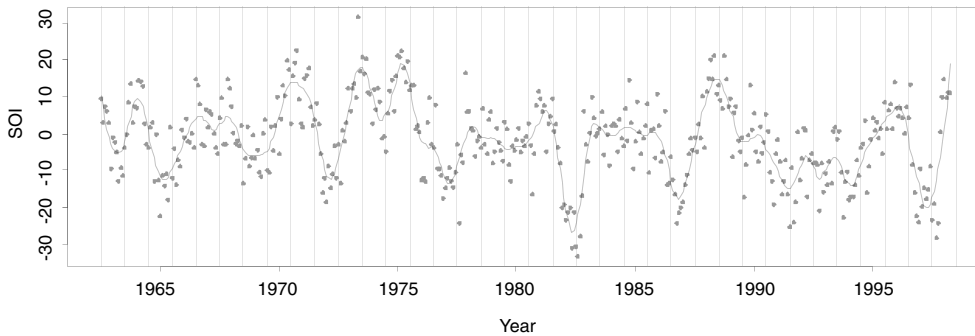


Figure 1. Monthly Southern Oscillation Index with smooth line highlighting the pattern.  
The smooth line was computed using a loess curve of degree 2 with span of 6%.

latter because it is faster computationally. Repetition of various aspects of the analyses using loess did not show any notable differences.

We also need to select the  $r + 1$  smoothing parameters for each of the occurrence and intensity models. As a guide to selecting these smoothing parameters, we use Akaike's Information Criterion (AIC), defined by  $AIC = \text{deviance} + 2k$  where  $k$  is the total number of degrees of freedom in the model. We have had mixed success in using the AIC as a bandwidth selection method. In Grunwald & Hyndman (1998) we showed that the AIC is optimal or nearly so for selecting the smoothing parameter when smoothing non-Gaussian time series, whereas the Bayesian Information Criterion (BIC) gives extreme oversmoothing (selecting very small degrees of freedom). For fitting GAMs, the BIC also tends to give extreme oversmoothing, and the AIC often suggests reasonable smoothing parameters. However, occasionally the AIC is minimized with smoothing parameters which do not appear to highlight the effect being modelled. Consequently, here we have used it as a guide rather than as an automatic bandwidth selector. When the AIC suggested reasonable smoothing parameters we used them; otherwise we subjectively selected the smoothing parameters to provide a model which highlighted the effect of interest.

#### 4. Modelling rainfall occurrence in Melbourne

To simplify the analysis of seasonality, we omitted the nine leap days from the series, although the leap day data were used as the lagged regressors on 1 March when it followed a leap day. As in Grunwald & Jones (2000), we used the log of previous rainfall values to improve the fit. Specifically, we used  $\log(y_{t-j} + c)$  for some  $c > 0$ . (Without this transformation, a variable bandwidth would be necessary due to the extreme skewness of  $Y_{t-1}$ .) For the GLMs fitted by Grunwald and Jones,  $c$  was chosen by maximum likelihood to be equal to 0.2. To facilitate comparisons between models, we have also used  $c = 0.2$  in this paper.

We included as a covariate the value of the Southern Oscillation Index (SOI), the standardized anomaly of the mean sea level pressure (MSLP) between Tahiti and Darwin. Let  $T_k$  denote the Tahiti MSLP for month  $k$ ,  $D_k$  denote the Darwin MSLP for month  $k$ , and let  $\Delta_k = T_k - D_k$  denote the difference. Then the monthly value of the SOI is calculated as  $I_k^* = 10(\Delta_k - \mu_k)/\sigma_k$  where  $\mu_k$  and  $\sigma_k$  denote the mean and standard deviation, respectively, of  $\{\Delta_i; i(\bmod 12) = k(\bmod 12)\}$ . This is known as the Troup SOI. Figure 1 shows the monthly values between January 1963 and September 1998. There is clearly a lot of

random variation in the measurement. We have highlighted the underlying trend with a loess curve of degree 2 and span 6%. Negative values of  $I_k^*$  indicate 'El Niño' episodes and are usually accompanied by sustained warming of the central and eastern tropical Pacific Ocean, a decrease in the strength of the Pacific trade winds, and a reduction in rainfall over eastern and northern Australia. Positive values of  $I_k^*$  are associated with stronger Pacific trade winds and warmer sea temperatures to the north of Australia (a 'La Niña' episode). Together these are thought to give a high probability that eastern and northern Australia will be wetter than normal. It should be noted that the effect of the Southern Oscillation is greater in Queensland and New South Wales than Victoria (Allan, Lindesay & Parker, 1996). We defined  $x_{1t} = I_t$  to be the value of the fitted loess curve at day  $t$ . (Almost identical results are obtained if  $I_t$  is calculated by linearly interpolating the raw values of  $I_k^*$ .)

We also included the covariate  $x_{2t} = S_t = t \pmod{365}$  to model the seasonal variation. The function  $g_{p+2}$  was constrained to be periodic; that is, we constrained  $g_{p+2}(S_t)$  to be smooth at the boundary between  $S_t = 365$  and  $S_t = 1$ .

Thus our occurrence model had

$$\mu_t(x_t) = \alpha_0 + \sum_{k=1}^p (\alpha_k j_{t-k} + g_k(\log(y_{t-k} + c))) + g_{p+1}(I_t) + g_{p+2}(S_t) + g_{p+3}(t).$$

Models with  $p = 1, 2, 3$  and 4 were fitted. The results were very similar for all  $p$  so we selected  $p = 1$  because it simplified the interpretation.

The smooth term involving  $I_t$  was not significantly different from a linear function and so  $g_2(I_t)$  was restricted to the linear function  $g_2(z) = \alpha_2 z$ . Because  $g_3(S_t)$  was a periodic function, we modelled it using a Fourier function of the form

$$g_3(S_t) = \sum_{k=1}^m \left( \alpha_{is} \sin\left(\frac{2\pi k S_t}{365}\right) + \alpha_{ic} \cos\left(\frac{2\pi k S_t}{365}\right) \right),$$

and selected the value of  $m$  using the AIC. (An alternative approach would be to use a periodic smoother.) The smooth terms  $g_1(Y_{t-1} + c)$  and  $g_4(t)$  were fitted using smoothing splines. The final model had  $\hat{\alpha}_1 = 0.26$  (se = 0.07),  $\hat{\alpha}_2 = 0.0088$  (se = 0.0023),  $m = 3$  in  $g_3(S_t)$  and smoothing parameters  $df_1 = 4.9$  and  $df_4 = 50$  where  $df_i$  denotes the degrees of freedom for the smooth function  $g_i$ . The value of  $df_1$  was chosen by minimizing the AIC, while the smoothing parameter for  $g_4(t)$  was selected to allow sufficient flexibility for modelling changes in the probability of occurrence over a period of two or three years.

The value of  $\alpha_2$  was significant (using a  $t$ -test at the 5% level). However, if the SOI term was omitted from the model and the other terms re-estimated, the deviance of the model did not change significantly (using a  $\chi^2$  test at the 5% level). This anomaly occurred because, if the SOI was omitted, the  $g_4(t)$  term could model the variation in the SOI. We chose to include the SOI because we were interested in assessing its effect on rainfall. The term  $g_1(y)$  was significantly different from linear ( $P = 0.009$  using a  $\chi^2$  test). We discuss the significance of the  $g_4(t)$  term later.

Figure 2 shows some results for the fitted model. The lower solid line is the estimate of the probability of rain following a dry day ( $y_{t-1} = 0$ ),

$$\Pr(J_t = 1 \mid Y_{t-1} = 0) = \ell(\alpha_0 + g_1(\log c) + g_2(I_t) + g_3(S_t) + g_4(t)).$$

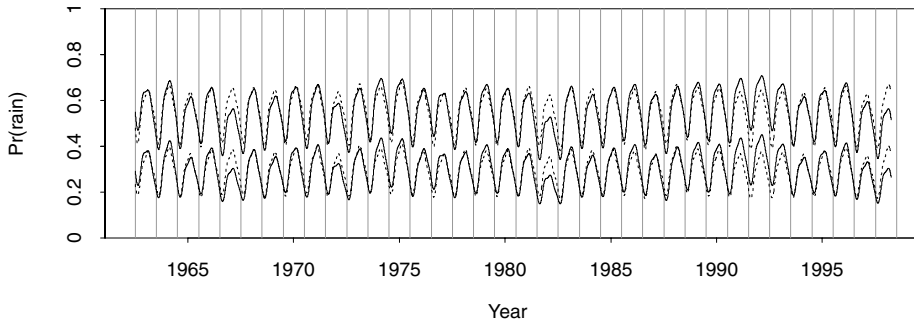


Figure 2. Lower solid line: estimated probability of rain following a dry day. Upper solid line: estimated probability of rain following a day of median intensity rainfall (2 mm). These estimates are based on the GAM; dashed lines show analogous curves for the GLM.

The upper solid line is the estimate of the probability of rain following a day of median intensity rainfall (2 mm),

$$\Pr(J_t = 1 \mid Y_{t-1} = 2) = \ell(\alpha_0 + \alpha_1 + g_1(\log(2 + c)) + g_2(I_t) + g_3(S_t) + g_4(t)).$$

For comparison, analogous curves for a GLM are shown as dashed lines. This model had

$$\begin{aligned} \mu_t(\mathbf{x}_t) = & \alpha_0 + \alpha_1 j_{t-1} + \alpha_1^* \log(y_{t-1} + c) + \alpha_2 I_t \\ & + \sum_{k=1}^3 \left( \alpha_{is} \sin\left(\frac{2\pi k S_t}{365}\right) + \alpha_{ic} \cos\left(\frac{2\pi k S_t}{365}\right) \right). \end{aligned}$$

Again, the AIC was used to select the number of sinusoidal terms in the seasonal pattern.

Higher order AR models were tried but gave very similar results. Note that the GAM allows the modelling of non-seasonal temporal variation whereas the GLM does not.

We can also look at the probability of rainfall occurrence as a function of the rainfall intensity of the previous day. Figure 3 shows this relationship with all other variables held fixed at the levels observed on two days in the period of the data. The lower curves are for 17 February 1982 (when  $g_2(I_t) + g_3(S_t) + g_4(t)$  was minimized). The upper curves are for 20 August 1992 (when  $g_2(I_t) + g_3(S_t) + g_4(t)$  was maximized). The solid lines represent the probabilities calculated using the GAM, conditioning on the value of  $t$ . The dashed lines show the analogous probabilities calculated using the GLM.

#### 4.1. Seasonally adjusted occurrence effects

One objective of the GAM analysis is to highlight unusual periods of occurrence, relative to ‘typical’ annual occurrence patterns. For instance, comparing the GLM and GAM fits in Figure 2 suggests that 1982 had unusually low occurrence and 1990–93 had unusually high occurrence. To facilitate and quantify such comparisons, we can apply a simple method of seasonal decomposition to decompose  $\mu_t(\mathbf{x}_t)$  into a seasonal term  $s_t(\mathbf{x}_t)$  that repeats each year and represents a ‘typical’ year, and a remainder term  $r_t(\mathbf{x}_t)$  that represents deviations

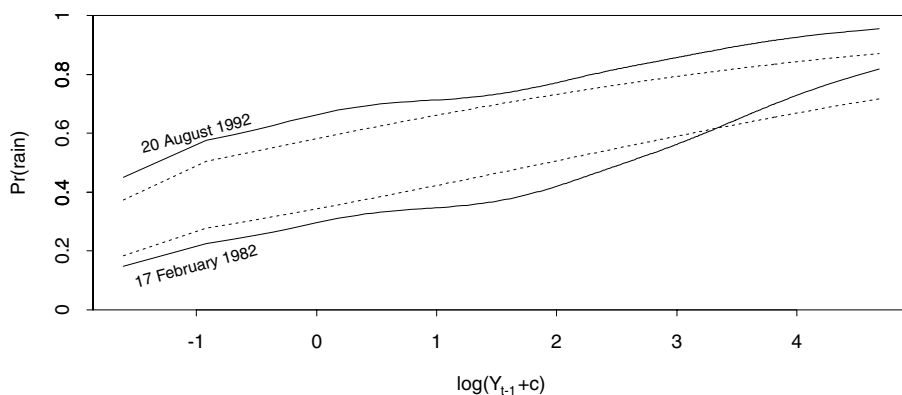


Figure 3. Lower solid line: estimated probability of rain vs.  $\log(Y_{t-1} + c)$  with all other variables held at the levels observed on 17 February 1982. Upper solid line: estimated probability of rain vs.  $\log(Y_{t-1} + c)$  with all other variables held at the levels observed on 20 August 1992. Dashed lines show analogous curves for the GLM.

from this regular pattern. Let  $\mu_t(\mathbf{x}_t) = s_t(\mathbf{x}_t) + r_t(\mathbf{x}_t)$  where  $s_t(\mathbf{x}_t) = s_{t+365k}(\mathbf{x}_t)$  for  $k = 1, 2, \dots$ . These effects can be interpreted in terms of odds of rain, so that

$$\frac{\Pr(J_t = 1 \mid \mathbf{X}_t = \mathbf{x}_t)}{\Pr(J_t = 0 \mid \mathbf{X}_t = \mathbf{x}_t)} = \exp(\mu_t(\mathbf{x}_t)) = \exp(s_t(\mathbf{x}_t)) \exp(r_t(\mathbf{x}_t)).$$

Thus  $\exp(r_t(\mathbf{x}_t))$  represents the factor deviation of the odds of rain from the odds in a typical year, at time  $t$ . The seasonally adjusted probability of rain is

$$\pi_t^a(\mathbf{x}_t) = \ell(\bar{s}(\mathbf{x}_t) + r_t(\mathbf{x}_t)),$$

where  $\bar{s}(\mathbf{x}_t) = \frac{1}{365} \sum_{t=1}^{365} s_t(\mathbf{x}_t)$ , and the seasonal probability of rain is

$$\pi_t^s(\mathbf{x}_t) = \ell(s_t(\mathbf{x}_t)).$$

Our model provided a convenient estimate of  $s_t(\mathbf{x}_t)$ . We let

$$\hat{s}_t(\mathbf{x}_t) = \hat{\alpha}_0 + \hat{\alpha}_1 \bar{j}_{t-1} + \bar{g}_1 + \hat{\alpha}_2 \bar{I} + \hat{g}_3(S_t) + \bar{g}_4,$$

where  $\bar{j}$  denotes the mean of  $j_t$ ,  $\bar{I}$  the mean of  $I_t$ ,  $\bar{g}_1$  denotes the mean of  $\hat{g}_1(\log(y_{t-1} + c))$  and  $\bar{g}_4$  the mean of  $\hat{g}_4(t)$ ,  $t = 1, \dots, n$ .

Figure 4 shows estimates of the seasonal probability of rain,  $\pi_t^s$ , and the seasonally adjusted probability of rain,  $\pi_t^a$ , plotted against time  $t$ . The most striking periods of low occurrence are in 1967, 1972, 1982 and 1998. Apart from the most recent drought, these are exactly the droughts in areas encompassing Melbourne, as reported by Keating (1992). The period of highest probability of occurrence is 1992 (which had the greatest number of wet days of any year in the period studied).

Our model attempted to separate the non-seasonal temporal variation,  $g_2(I_t) + g_4(t)$ , into two parts: one due to the SOI and one which was unaffected by the SOI. To help visualize the

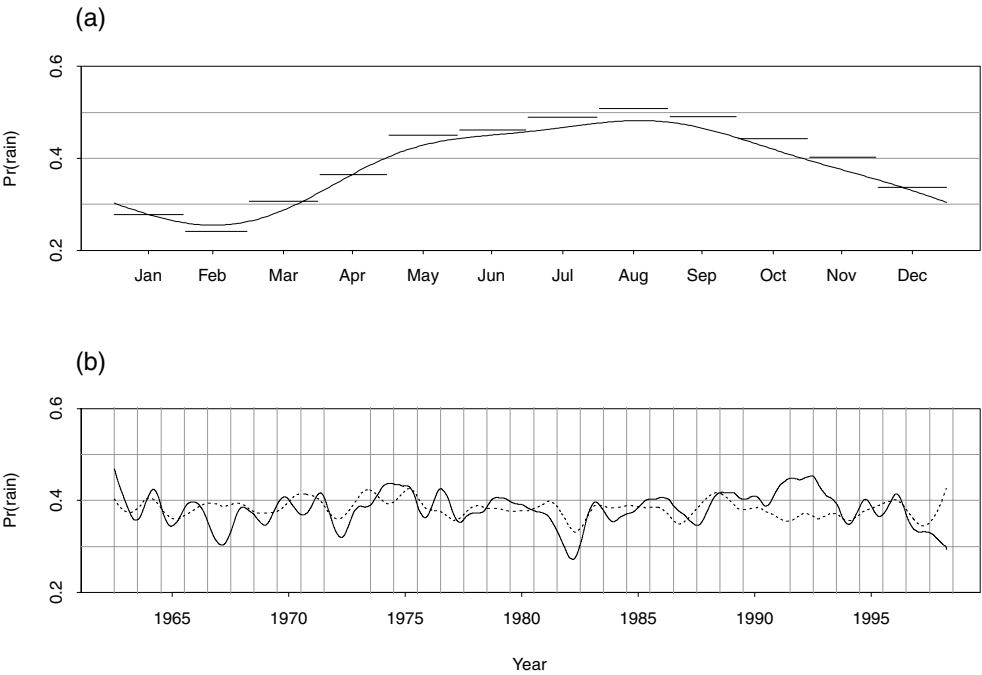


Figure 4. (a) Estimated seasonal probability of rain,  $\pi_t^s$ . The horizontal bars show the proportion of rainy days for each month during the data period. (b) Seasonally adjusted estimated probability of rain,  $\pi_t^a$ . The dashed lines shows the estimated probability of rain further adjusted to show the effect of the SOI.

effect of this separation, the dashed lines in the bottom graph of Figure 4 show the probability of rain predicted by the model after seasonal adjustment and removing the effect of  $g_4(t)$ . That is, we have graphed

$$\ell(\hat{s}_t(x_t) + \hat{\alpha}_2(I_t - \bar{I})).$$

The resulting curve shows the effect of the SOI on rainfall probability.

The differences between the solid and dashed curves are of interest. For example, in 1967, the solid curve is substantially lower than the dashed curve. This was a period of drought (reflected by the dip in the solid curve) which was not associated with a corresponding low in the SOI. The drought of 1982 was associated with the SOI (hence the trough in the dashed curve), but it was more severe than the SOI suggested. Thus, the solid line dips further than the dashed line. The period 1991–93 was one with unusually high rainfall occurrence that was not associated with a corresponding high in the SOI.

Much of the non-seasonal temporal variation in rainfall probability is being modelled by  $\hat{g}_4(t)$  rather than  $g_2(I_t)$ . So while the SOI appears to have some effect on the rainfall occurrence it is not a strong predictor and extreme values of the SOI do not always translate into extreme values of rainfall probability in the Melbourne area.

It should be noted that not all of the wiggles in the seasonally adjusted probabilities are likely to be ‘real’. To assess the importance of the features of the curve, we calculated pointwise confidence intervals around  $\hat{g}_4(t)$ , the greatest contributor to the fluctuations in the seasonally adjusted probabilities. These are shown in Figure 5. The confidence intervals were calculated using plus and minus twice the pointwise standard error of  $\hat{g}_4(t)$ , calculated as



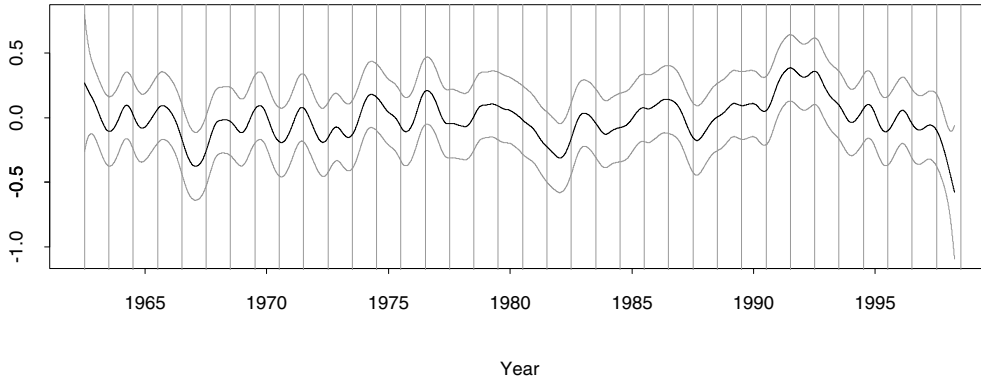


Figure 5. The curve  $\hat{g}_4(t)$  with pointwise 95% confidence intervals calculated using plus and minus twice the standard error

described in Hastie & Tibshirani (1990 p.60). It seems that the major troughs such as those in 1967, 1982 and 1998 are genuine drops in rainfall probability, whereas some of the smaller wiggles such as those in 1973 and 1995 are probably artefacts of the data.

## 5. Modelling intensity

Following the same sorts of modelling procedures as we used for the occurrence process, we can construct GLMs and GAMs for rainfall intensity  $W_t$ . Recall that  $W_t = Y_t$  if  $Y_t > 0$ , and that we assumed it had distribution  $G(\nu_t(\mathbf{x}_t), r)$  where  $G(\nu, r)$  denoted a Gamma distribution with mean  $\nu > 0$  and shape parameter  $r > 0$ . The fitted model had conditional mean

$$\nu_t(\mathbf{x}_t) = \exp(\beta_0 + \beta_1 j_{t-1} + h_1(y_{t-1} + c) + \beta_2 I_t + h_3(S_t) + h_4(t)).$$

(As with occurrence, we also tried higher order autoregressive terms but they made little difference to the fitted models.) The seasonal term  $h_3$  had  $m = 4$  and the bandwidths for  $h_1(y_{t-1})$  and  $h_4(t)$  were 14 and 50, respectively ( $df_1$  chosen by minimizing the AIC). The estimated coefficients were  $\hat{\beta}_1 = -0.18$  (se = 0.07) and  $\hat{\beta}_2 = 0.0094$  (se = 0.0023). The curve  $h_1$  was significantly different from linear ( $P = 0.018$  using an  $F$ -test). Figure 6 shows pointwise 95% confidence intervals around  $\hat{h}_4(t)$ , indicating that the major ‘dips’ in rainfall intensity in 1967, 1975–76 and 1996 are significant.

Interestingly, the drought of 1982 does not appear to have affected rainfall intensity — it apparently was an event mainly involving the frequency of rain, not the amount of rain when it rained. The summer of 1996–97 had unusually low rainfall intensity, whereas it was not unusual in its frequency of rain (compare Figure 2). While both years were associated with an El-Niño event (indicated by low values of the SOI, see Figure 1), the effect appears to have been different.

Residual analysis for this model is possible using the scaled data  $R_t = W_t/\nu_t(\mathbf{x}_t)$ . Then, if the model is correct,  $R_t \stackrel{d}{=} G(1, r)$ . So plots of  $\hat{R}_t$  against predictors and QQplots of  $\hat{R}_t$  against the quantiles of a  $G(1, \hat{r})$  distribution (as discussed in Grunwald & Jones, 2000) permit some assessment of the fitted model. For the model fitted here, these residual plots did not reveal any model inadequacies.

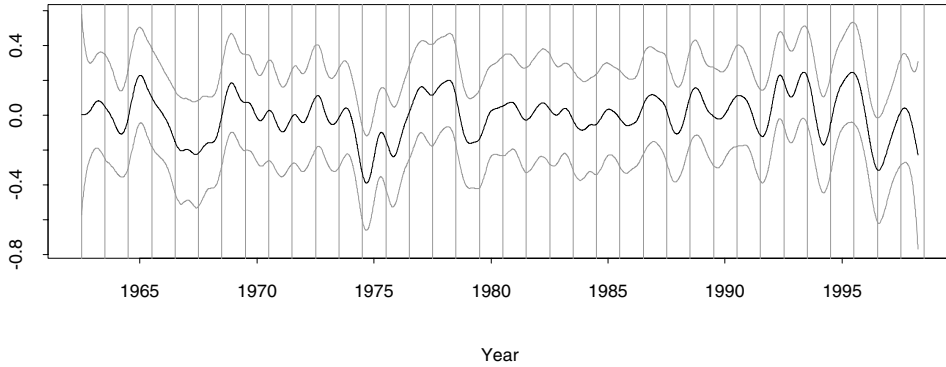


Figure 6. The curve  $\hat{h}_4(t)$  with pointwise 95% confidence intervals calculated using plus and minus twice the standard error

The GLM we used had

$$\begin{aligned} \nu_t(\mathbf{x}_t) = \exp & \left( \beta_0 + \beta_1 j_{t-1} + \beta_1^* \log(y_{t-1} + c) + \beta_2 I_t \right. \\ & \left. + \sum_{k=1}^4 \left[ \beta_{ks} \sin\left(\frac{2\pi k S_t}{365}\right) + \beta_{kc} \cos\left(\frac{2\pi k S_t}{365}\right) \right] \right). \end{aligned}$$

The sinusoidal terms describe the seasonal pattern in rainfall intensity. The number of sinusoidal terms was chosen using the AIC.

Figure 7 shows the mean rainfall intensity  $\nu_t(\mathbf{x}_t)$  plotted against  $t$  for two different values of  $y_{t-1}$ . The top plot shows the curve following a dry day ( $y_{t-1} = 0$ ). For comparison, the analogous curve from the fitted GLM is shown. The bottom plot shows the curve where the previous day had rainfall  $y_{t-1} = 30.2$  mm. This value of  $y_{t-1}$  provides the maximum value of  $\hat{h}_1$ . The GLM curve in the lower plot is clearly biased downwards due to the assumption of a linear relationship with  $\log(y_{t-1} + c)$ .

Figure 8 shows the mean rainfall intensity as a function of  $\log(y_{t-1} + c)$ . The values of the other variables were held fixed at the levels observed on day  $t$  where  $t$  was chosen to provide the minimum and maximum values of  $\hat{h}_2(I_t) + \hat{h}_3(S_t) + \hat{h}_4(t)$ . The amount of rain on one day,  $y_{t-1}$ , had virtually no effect on the amount of rain on the subsequent day,  $y_t$ , unless  $y_{t-1} > e^3 - c \approx 20$  mm. In other words, there is little autocorrelation in the intensity series unless there is a large rainstorm, in which case it probably extends into the following day. The nonlinear relationship demonstrates why there is bias in the GLM estimate of intensity as seen in Figure 7.

The seasonally adjusted mean intensity was calculated in a way similar to that for probability of occurrence described in Section 4.1. The results are shown in Figure 9. Of the major droughts, not all are clearly identified by low intensity. The droughts of 1967 and 1982 were periods of low intensity but not the drought of 1972. Although the SOI is statistically significant, its effect is small. The major non-seasonal temporal variation in intensity is not associated with the SOI.

## 6. Markov generalized additive models for rainfall

We now consider combining the occurrence and intensity models of previous sections to give a model for rainfall amount with a mixed density as given in (2.1). In some applications

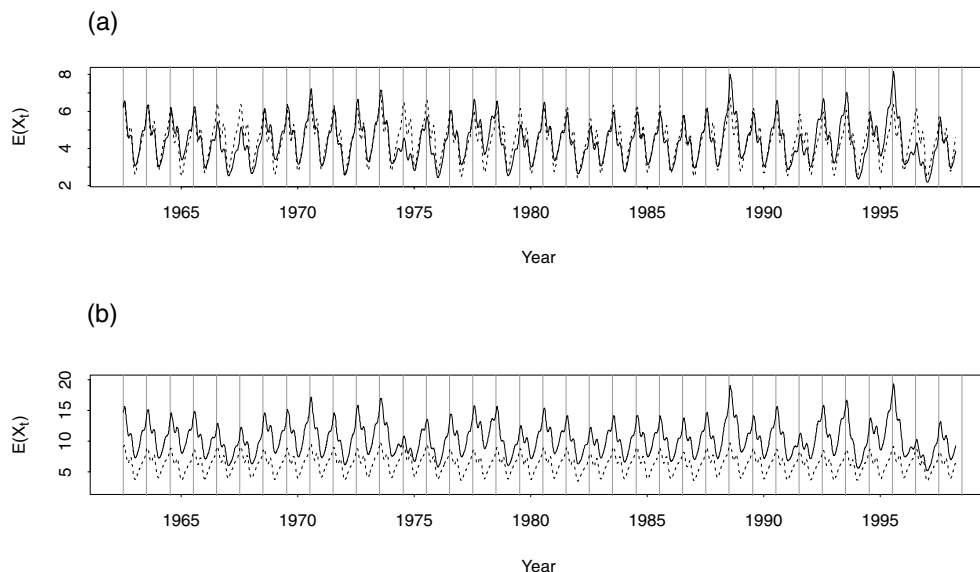


Figure 7. (a) Estimated mean intensity of rain following a dry day. Solid lines calculated from the GAM, dashed lines calculated from the GLM. (b) Estimated mean intensity of rain following a day with 30.2 mm of rain. Solid lines calculated from the GAM, dashed lines calculated from the GLM. Note that the vertical scales on these two plots are not the same.

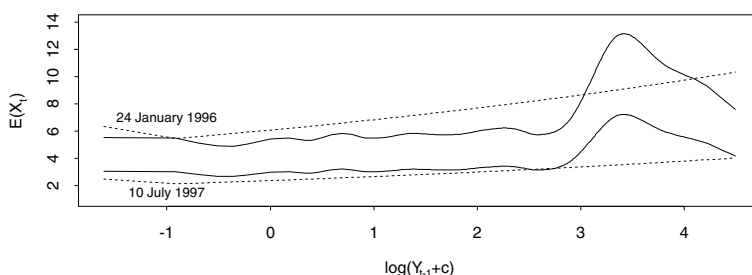


Figure 8. Mean rainfall intensity (calculated from the GAM) vs  $\log(Y_{t-1} + c)$  with all other variables held at the levels observed on two days: 24 January 1996 and 10 July 1997. These days were at the maximum and minimum of  $\hat{h}_2(I_t) + \hat{h}_3(S_t) + \hat{h}_4(t)$  respectively. Solid lines calculated from the GAM; dashed lines calculated from the GLM.

this combined model is of most interest, because it has units of mm/day while intensity has units of mm/wet day. The fitted amount model yields a mixed density which can be summarized in various ways. For instance, we can calculate the mean of  $Y_t$  directly from (2.1) as

$$E(Y_t | \mathbf{X}_t = \mathbf{x}_t) = \pi_t(\mathbf{x}_t)v_t(\mathbf{x}_t).$$

We are also interested in the marginal mean

$$M_t = E(Y_t | X_{1t} = x_{1t}, \dots, X_{r-p,t} = x_{r-p,t}),$$

although this is difficult to calculate analytically from the fitted model. Instead we have simulated 10000 sample paths from the model and average across the sample paths to calculate  $\hat{M}_t$ .

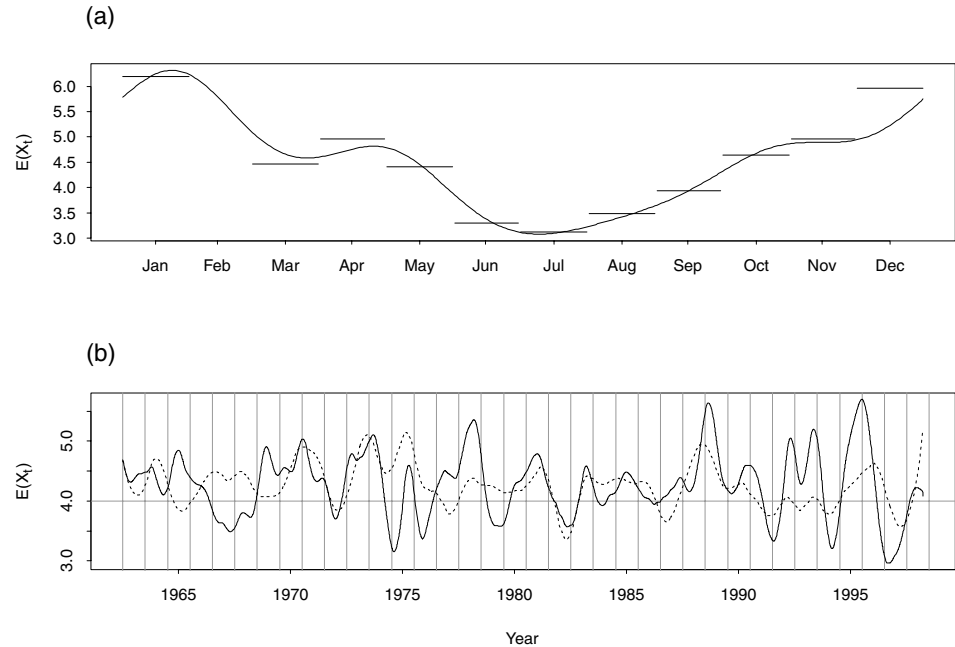


Figure 9. (a) Seasonal mean intensity. The horizontal bars show the average rainfall intensity for each month during the data period. (b) Seasonally adjusted mean intensity. The dashed lines shows the probability of rain further adjusted to show the effect of the SOI.

To find the seasonally adjusted mean of  $Y_t$ , we let  $\hat{s}_t^* = \text{average}(\hat{M}_{t+365k})$  for  $t = 1, \dots, 365$  and the average was taken over  $k = 0, \pm 1, \pm 2, \dots$ . Then we smoothed  $\hat{s}_t^*$  using a periodic smoother to obtain  $s_t$ , the average rainfall for day  $t$ . Finally, the seasonally adjusted rainfall on day  $t$  was  $r_t = M_t - s_t + \bar{s}_t$ . The results are shown in Figure 10 with the seasonal average ( $s_t$ ) shown in the top graph and the seasonally adjusted values ( $r_t$ ) shown in the bottom graph.

Note that there is far less variability in the seasonal mean amount than in the seasonal probability of occurrence or seasonal mean intensity. The probability of occurrence is highest in the winter months while the mean intensity is highest in the summer months. These seasonal patterns largely cancel each other out to give a relatively flat daily mean amount across the year. However, the probability density of rainfall amount varies a lot throughout the year, even though the mean is relatively stable. This is seen, for example, in the conditional distribution functions shown in Grunwald & Jones (2000).

The seasonally adjusted values show that droughts in southern Victoria are more complex than may have previously been understood. Comparing Figures 4, 9 and 10, we note that the drought of 1994, for example, appears to have resulted from lower intensity than usual but that the occurrence was not particularly low for that year. However, the drought of 1982 appears to be due more to low occurrence than to low intensity.

Crude estimates of the seasonally adjusted mean curves for amount, intensity and occurrence can be obtained by relatively simple smoothing techniques. However, the modelling approach we have used here has enabled us to go much further in estimating curves conditional on past observations, in estimating the effect of the SOI on both occurrence and intensity, and in decoupling the effects of occurrence and intensity on rainfall amounts.

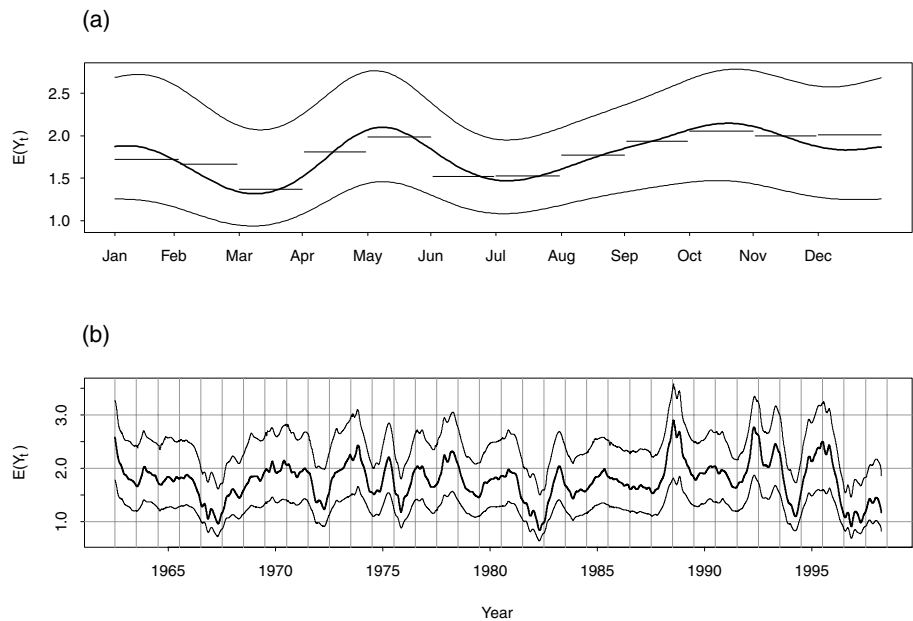


Figure 10. (a) Seasonal mean amount. (b) Seasonally adjusted mean amount. The lower curves show mean, conditional on previous day being dry; the upper curves show mean conditional on previous day having median intensity rainfall (2 mm); the centre (bold) curves show unconditional means. The horizontal lines show the average amount for each month in the data period.

TABLE 1  
*LDS = length of dry spell (days)*  
*Observed and expected numbers of dry spells over the period of the data*

LDS	3	4	5	6	7	8	9	10	11	12	13	14	≥ 15
Obs	307	239	156	104	81	41	33	30	30	14	14	10	37
Exp	197	162	128	105	89	70	60	49	43	33	31	23	160

The purpose of our model has been to investigate the effects of temporal variation and of covariates such as the SOI on rainfall. We have not attempted to provide an all-purpose model for investigating other aspects of rainfall. For example, our model does not perform well for modelling dry spells. Table 1 shows the actual number of dry spells of different lengths observed in the data, and the number predicted by the model. These predictions were obtained by simulating 50 sample paths from the model and computing the number of dry spells of each length for each sample path. The numbers were then averaged to give the values in the table. The standard errors for these predicted values are less than 2.0 in all cases. Inclusion of higher order AR terms might lead to better dry spell prediction.

However, the model has implications for long-term forecasting because it attempts to describe the relationship between precipitation and other explanatory variables over a long period of time. To produce such forecasts, we must estimate the conditional mean functions for the occurrence and intensity models for future times.

This can be done by simulating future sample paths from the model, and then averaging these at each time point. Where  $x_{i-p,t}$  is not known in advance (such as with the SOI), it must

be replaced by a forecast or by a given value representing a situation of interest. The non-seasonal temporal variation must also be forecast because the functions  $g_{r+1}(t)$  and  $h_{r+1}(t)$  are not defined for  $t$  beyond the range of the historical data. These can be computed by fitting stationary AR models. This approach has two advantages: (1) being able to model the cyclic fluctuations seen in the models for Melbourne's rainfall, and (2) producing long-term forecasts which converge to the long-term mean (see Makridakis, Wheelwright & Hyndman, 1998).

Until recently, the Bureau of Meteorology used forecasts of the SOI to guide their long-term climate prediction. The analysis presented here suggests that this procedure is not going to yield good prediction for southern Victoria because the relationship between the SOI and rainfall is not strong. The method is probably much better for locations in New South Wales and Queensland where the relationship between the SOI and rainfall is stronger (Allan, Lindesay & Parker, 1996). However, even there the model presented here probably leads to better long-term forecasts because it incorporates temporal variation not due to the SOI.

The current practice of the Bureau of Meteorology in long-term rainfall prediction (Drosowsky & Chambers, 1998) is to use rotated principal components of sea surface temperature anomalies recorded at sites in the Indian and Pacific oceans. We have not attempted to use those data in our model, but the analysis presented here suggests a new method which could be used with those predictors to produce more accurate long-term climate prediction.

The model, as presented here, is less useful for short-term forecasting. That would be better handled spatially rather than restricting attention to a single station, and would involve other meteorological covariates. The extension to a spatial network is an open problem.

### References

- AITCHISON, J. (1955). On the distribution of a positive random variable having a discrete probability mass at the origin. *J. Amer. Statist. Assoc.* **50**, 901–908.
- ALLAN, R., LINDESAY, J. & PARKER, D. (1996). *El Niño: Southern Oscillation and Climatic Variability*. Melbourne, Australia: CSIRO Publications.
- CLEVELAND, W.S., GROSSE, E. & SHYU, W.M. (1992). Local regression models. In *Statistical Models in S*, eds J.M. Chambers & T.J. Hastie. Pacific Grove: Wadsworth and Brooks.
- DROSDOWSKY, W. & CHAMBERS, L. (1998). *Near Global Sea Surface Temperature Anomalies as Predictors of Australian Seasonal Rainfall*. Research Report No. 65. Melbourne, Australia: Bureau of Meteorology Research Centre.
- EILERS, P.H.C. & MARX, B.D. (1996). Flexible smoothing with B-splines and penalties (with discussion). *Statist. Sci.* **89**, 89–121.
- GREEN, P.J. & SILVERMAN, B.W. (1994). *Nonparametric Regression and Generalized Linear Models: a Roughness Penalty Approach*. London: Chapman and Hall.
- GRUNWALD, G.K. & HYNDMAN, R.J. (1998). Smoothing non-Gaussian time series with autoregressive structure. *Comput. Statist. Data Anal.* **28**, 171–191.
- GRUNWALD, G.K. & JONES, R.J. (2000). Markov models for time series with mixed distribution. *Environmetrics* **11** (in press).
- HASTIE, T.J. & TIBSHIRANI, C. (1990). *Generalized Additive Models*. London: Chapman and Hall.
- HYNDMAN, R.J. & YAO, Q. (1998). Nonparametric estimation and symmetry tests for conditional density functions. Working paper. Department of Econometrics and Business Statistics, Monash University.
- HYNDMAN, R.J., BASHTANNYK, D.M. & GRUNWALD, G.K. (1996). Estimating and visualizing conditional densities. *J. Comput. Graph. Statist.* **5**, 315–336.
- KATZ, R.W. & PARLANGE, M.B. (1995). Generalizations of chain-dependent processes: applications to hourly precipitation. *Water Resources Research* **31**, 1331–1341.
- KEATING, J. (1992). *The Drought Walked Through: a History of Water Shortage in Victoria*. Melbourne: Department of Water Resources Victoria.
- MAKRIDAKIS, S., WHEELWRIGHT, S.C. & HYNDMAN, R.J. (1998). *Forecasting: Methods and Applications*. New York: John Wiley & Sons.
- McCULLAGH, P. & NELDER, J. (1989). *Generalized Linear Models*, 2nd edn. London: Chapman and Hall.
- STERN, R.D. & COE, R. (1984). A model fitting analysis of daily rainfall data (with discussion). *J. Roy. Statist. Soc. Ser. A* **147**, 1–34.